Template-Directed Assembly of Receptor Signaling Complexes[†]

Anthony L. Shrout, David J. Montefusco, and Robert M. Weis*

Department of Chemistry, LGRT 701, 710 North Pleasant Street, University of Massachusetts, Amherst, Massachusetts 01003-9336

Received July 18, 2003; Revised Manuscript Received September 26, 2003

ABSTRACT: Transmembrane receptors in the signaling pathways of bacterial chemotaxis systems influence cell motility by forming noncovalent complexes with the cytoplasmic signaling proteins to regulate their activity. The requirements for receptor-mediated activation of CheA, the principal kinase of the *Escherichia coli* chemotaxis signaling pathway, were investigated using self-assembled clusters of a receptor fragment (CF) derived from the cytoplasmic domain of the aspartate receptor, Tar. Histidine-tagged Tar CF was assembled on the surface of sonicated unilamellar vesicles via a lipid containing the nickel-nitrilotriacetic acid moiety as a headgroup. In the presence of the adaptor protein CheW, CheA bound to and was activated ∼180-fold by vesicle-bound CF. The extent of CheA activation was found to be independent of the level of covalent modification on the CF. Instead, the stability of the complex increased significantly as the level of covalent modification increased. Surface-assembled CF was also found to serve as a substrate for receptor methylation in a reaction catalyzed by the receptor methyltransferase, CheR. Since neither CheA activation nor CF methylation was observed in comparable samples in the absence of vesicles, it is concluded that surface templating generates the organization among CF subunits required for biochemical activity.

The organization and asymmetry inherent in cell membranes creates an environment in which receptor proteins can effectively convey information between the inside and the outside of the cell (*1*). The reduction in the degrees of freedom experienced by transmembrane and peripheral membrane proteins provides a strong driving force for lateral organization, which can be essential for function (e.g., ligand-induced clustering (*2*)). These factors are in effect at the plasma membrane inner leaflet, where the assembly and regulation of signaling components often occur (*3*−*5*). In the chemotaxis signal transduction pathway of *Escherichia coli*, complexes of transmembrane receptors and cytoplasmic signaling proteins (*6*, *7*) regulate protein phosphorylation through ligand−receptor interactions and receptor covalent modification (*8*−*14*). This transduction pathway is coupled to cell motility, which biases the swimming behavior of the cell in attractant and repellant gradients (*15*).

Several lines of evidence suggest that receptors for the bacterial chemotaxis pathway in *E. coli* are clustered in the cell membrane (*16*−*18*) and that close associations between receptors of different ligand specificity are important in signaling (*19*−*23*). This large class of bacterial receptors (*24*, *25*) is also known as the methyl-accepting chemotaxis proteins (MCPs),[1] due to the enzyme-catalyzed receptor methylation and demethylation reactions that are essential for sensory adaptation (*26*). A structural model for the MCP dimer, which has been generated by Kim et al. from the crystal structures of the soluble domains (*27*), is shown in Figure 1 and provides insights into the molecular basis for the requirement of receptor clusters in signaling. *E. coli* has four MCPs (Tar, Tsr, Tap, and Trg) and an aerotaxis receptor (Aer), which are distinguished primarily by ligand binding specificities that reside in the N-terminal domains. The dimeric organization of MCPs is evident in crystal structures of the aspartate receptor (Tar) ligand binding domain (*28*, *29*) and the serine receptor (Tsr) cytoplasmic domain (*27*). The significantly greater homology among the C-terminal domains of these five receptors provides the basis for common interactions among a set of cytoplasmic signaling proteins (*24*), which generate the excitatory and adaptive responses to the chemotactic stimuli (reviewed in ref *30*). In addition, the Tsr cytoplasmic domain is organized as a trimer-of-dimers in the crystal structure (*27*). The subunit interactions that lead to the trimer-of-dimer structure are apparently important for the intact receptor in the cell since mutations in conserved amino acid residues at the trimer-of-dimer contact site disrupt chemotaxis and receptor clustering (*23*). Thus, within the context of these heterogeneous receptor clusters, the overall CheA activity reflects the influences of the various independent inputs detected by the MCPs and Aer.

Biochemical investigations using membrane preparations of either Tar or Tsr with the purified signaling proteins have

[†] This work was supported through the NIH grant R01 GM53210 (R.M.W.).

* To whom correspondence should be addressed. Phone: (413) 545-0464. Fax: (413) 545-4490. E-mail: rmweis@chem.umass.edu.

[1] Abbreviations: MCP, methyl-accepting chemotaxis protein; Tar, aspartate receptor; Tsr, serine receptor; Tap, dipeptide receptor; Trg, ribose/galactose receptor; Aer, aerotaxis receptor; CF, cytoplasmic fragment; DOPC, 1,2-dioleoyl-*sn*-glycero-3-phosphocholine; DOGS-NTA, 1,2-dioleoyl-*sn*-glycero-3-{[*N*(5-amino-1-carboxypentyl)iminodiacetic acid]-succinyl} ammonium salt); DOGS-NTA-Ni^{2+}, DOGS-NTA nickel salt; SUV, sonicated unilamellar vesicles; Ni-NTA, nickel-nitrilotriacetic acid; *tod*, trimer-of-dimer; SAM, *s*-adenosyl-L-methionine.

10.1021/bi0352769 CCC: $25.00
Published on Web 10/28/2003

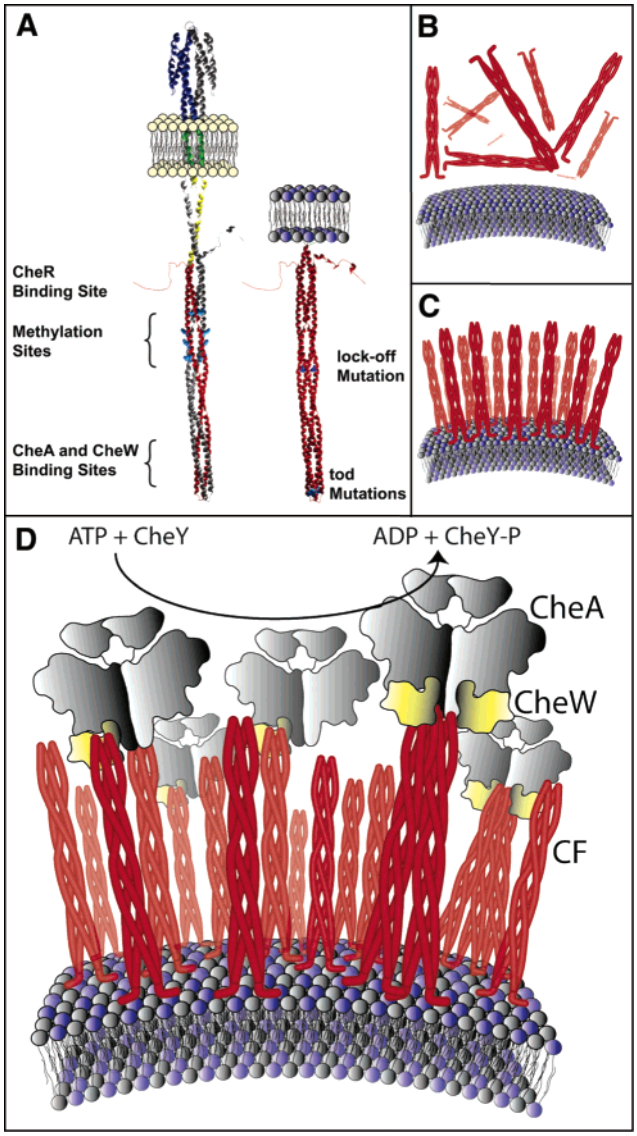

FIGURE 1: Receptor structure and surface-templated complex assembly. (A) The model of the chemotaxis receptor dimer at left is based primarily on the ligand binding and cytoplasmic domain crystal structures (*27*). One subunit is rendered in gray, and the other is color-coded to indicate functional regions: ligand binding domain (blue), transmembrane segments (green), linker region (yellow), and the cytoplasmic domain (red). The methylation sites (Q295, E302, Q309, and E491) are depicted with space-filling representations. The membrane-anchored CF dimer at right indicates positions of the S461L *lock-off* mutation and two *tod* mutations (E383A and E382P) in space-filling representation. (B−D) Cartoons depicting CF binding to the SUV surface. CFs are shown as dimers for simplicity.

clarified some of the properties of CheA activation and regulation (*8*−*14*). Notable observations include the substantial increase in CheA activity (>100-fold) that accompanies signaling complex formation, the stimulating influence of receptor methylation on CheA activity, and the inhibitory influence of ligand binding. However, membrane samples of the MCPs that are used in these biochemical experiments are frequently isolated from cells expressing the receptor at elevated levels, which can result in complex and heterogeneous samples (*31*). In addition, receptor reconstitution is labor-intensive, and the conditions that maintain a high level of activity while also preserving the vectoral and lateral organization required for function can be difficult to find (*32*, *33*). To circumvent the difficulties that typically plague the use of such samples, studies of CheA activation have used soluble receptor cytoplasmic fragments (CFs). In many instances the CFs are unable to activate CheA, but those that do activate CheA seem to do so via oligomerization, which occurs synergistically with CheW and CheA binding (*34*−*37*). While this approach has helped to elucidate the enzymatic properties of receptor signaling complexes, the formation of these complexes is limited to certain relative concentrations of CF, CheW, and CheA and is undesirably sensitive to variations in the tendency of different CFs to oligomerize. As a result, it has not been possible to study all the factors that are important for CheA activation.

We have developed a different approach for assembling signaling complexes that does not depend strongly on the propensity of the CF to self-associate, which has thus allowed us to study the formation of signaling complexes over a wide range of CheW concentrations. Sonicated unilamellar vesicles (SUVs) containing a nickel-chelating lipid (*38*) were used to template the assembly of histidine-tagged CF derived from *E. coli* Tar onto the outer leaflet of the membrane bilayer. The organization of CF produced by vesicle binding was found to resemble the environment of the cell membrane inner leaflet sufficiently well to promote the assembly of active (CF/CheW/CheA) signaling complexes and to restore enzyme-catalyzed methylation of the CF. The vesicle templating approach described here promises to be generally useful in situations where the signaling proteins require the organizing influence of the cell membrane to function.

MATERIALS AND METHODS

Protein Purification. The chemotaxis proteins CheA, CheR, CheW, CheY, and Tar CF were purified according to established protocols (*11*, *19*, *39*). Tar CF was expressed from the plasmid pHTCF (*19*), which generated a protein that contains residues 257−553 of *E. coli* Tar, a vector-encoded hexahistidine affinity tag at the N-terminus ($MRGSHHHHHHGSPM_{257}$), and the wild-type pattern of amidation (QEQE) at the methylation sites (Gln295, Glu302, Gln309, Glu491). pHTCF derivatives pSM100 and pSM101, which were used to produce CF in the deamidated (CF_{EEEE}) and fully amidated (CF_{QQQQ}) forms, respectively, were constructed with standard site-directed mutagenesis methods and verified by sequencing. Protein concentrations were determined with the Lowry assay according to the manufacturer's instructions (D_c Protein Assay, Bio-Rad Laboratories). Purified and concentrated proteins were flash frozen in liquid nitrogen and stored at −75 °C.

Assembly of Vesicle-Templated Signaling Complexes. SUVs were prepared from chloroform solutions of DOGS-NTA-Ni^{2+} and DOPC (Avanti Polar Lipids) in a 1:1 molar ratio, which were evaporated under a nitrogen stream until a dried lipid film was obtained. Assay buffer (pH 7.5, 75 mM Tris-HCl, 100 mM KCl, 5 mM $MgCl_2$, 2 mM TCEP, 5% DMSO) was added to produce a 2 mg/mL lipid concentration, the film was hydrated for 20 min at 25 °C, and then the sample was bath sonicated at 30 °C (Branson Model 2510) until the solution clarified (∼70 min). Isothermal titration calorimetry was used to estimate that 60% of the DOGS-NTA-Ni^{2+} was in the outer leaflet of the SUV membrane and available for CF binding (data not shown).

This value was determined from the relative endpoints of titrations between nickel and SUVs containing DOGS-NTA using a matched pair of samples, one in buffer (outer leaflet accessible) and the other in buffer plus 1% octyl glucoside (all sites accessible). Vesicle-bound signaling complexes were generated in a 75 μL sample volume by incubating vesicles (280 μM in DOGS-NTA-Ni^{2+}) and 30 μM CF in assay buffer for 2 min at 25 °C, followed by the addition of CheA (1.2 μM) and CheW (0−35 μM) with gentle vortexing and incubation at 25 °C for 3.5 h.

Vesicle samples were analyzed for signal complex formation by separating the vesicle-bound protein using sedimentation (125 000*g* for 15 min in a Beckman TLX centrifuge with a TLA-120.2 rotor). Samples of free (supernatant) and total protein (an aliquot removed prior to sedimentation) were analyzed on 15% SDS−polyacrylamide gels (BioWhittaker Molecular Sciences) with software-assisted scanning densitometry (GS-700 Densitometer, Molecular Analyst, version 1.4, Bio-Rad Laboratories).

Enzyme Assays. CheA-CheY phosphotransferase activity was measured in a steady-state coupled spectrophotometric ATPase assay (*40*, *41*) on 2 μL aliquots withdrawn from the samples (incubated for ∼3.5 h at 25 °C). ATPase activities were measured immediately (30 s) after diluting the aliquots 100-fold into buffer with 50 μM CheY and assay reagents (2.5 mM PEP, 4.0 mM ATP, 250 μM β-NADH, and 4 units of PK/LDH enzymes, obtained from Sigma-Aldrich). Specific activities (s^{-1}), defined as the turnover number per mole of CheA subunits in the sample, were determined from the absorbance change at 340 nm ($d[ADP]/dt = -6220\ dA_{340}/dt$). The activity of 50 μM CheY samples was subtracted as background. The extent of CheA activation was expressed relative to the activity of 5.0 μM CheA (0.074 s^{-1}), which was regarded as the solution activity of dimeric CheA. Normalized activities (s^{-1}) were computed for each of the samples from the specific activities and the fractions of CheA bound to vesicles.

The ability of CF to act as substrate for CheR was tested using 30 μM CF_{EEEE} incubated with vesicles (1:1 DOPC: DOGS-NTA-Ni^{2+}, 560 μM total lipid). Reactions were initiated by the addition of CheR and SAM at final concentrations of 6 μM and 10 mM, respectively. The 20 μL aliquots were removed at 0.1, 0.5, 2, 3, and 4.5 h, quenched in the course of preparing the samples for SDS−PAGE analysis, and resolved on 12.5% gels. The extent of the CF methylation reaction was estimated by the appearance of a protein band of increased mobility using densitometry, which is a known result of receptor methylation (*9*).

Curve Fitting. Nonlinear least-squares (NLS) fits of the CheA activity (Act) and vesicle-bound CheA (f_B) data were conducted in Origin version 7.0 (OriginLab Corporation, Northampton, MA) to specific models described in the Results. The parameters were adjusted iteratively in the NLS fitting engine of Origin by the Levenberg−Marquardt method until the errors were minimized (*42*).

RESULTS

Figure 1 illustrates the scheme used to generate CF/CheW/CheA complexes with the vesicle-templating approach. For simplicity, the CF is depicted in the coiled−coil hairpin dimer arrangement found in the X-ray structure (*27*) (Figure 1A), although the extent of CF dimerization in solution and on the surface is not known. CF is depicted to be randomly distributed in solution (Figure 1B) but orients on binding to a vesicle outer surface via the Ni-NTA−histidine interaction, possibly as depicted in Figure 1C. The CF orientation in Figure 1C is consistent with the observation of complete binding to vesicles (>95% of the CF cosediments with vesicles), which reasonably excludes other orientations requiring a larger area per CF molecule bound (i.e., side-on vs end-on binding).[2] Ternary complexes of CF, CheW, and CheA are then formed on the vesicle surface, and the CheA phosphotransferase activity is measured in the presence of excess CheY in a coupled steady-state ATPase assay (Figure 1D).

Activation of CheA by Surface-Assembled CF. The histogram of CheA activity in Figure 2A shows the effect of surface anchoring on CheA activity. CheA activity is significantly larger in the presence of Ni-NTA-SUVs as compared to samples without vesicles, irrespective of the level of covalent modification on the CF. The trend of increasing the specific activity with increasing levels of covalent modification, which is mimicked by replacing glutamates, E, with glutamines, Q, at the methylation sites (*47*), has been observed in previous studies of ternary (receptor−CheW−CheA) complexes formed with intact receptor molecules (*9*−*14*) and has been attributed to variations in the degree of CheA activation within the complex. The data in Figure 2 are at odds with this interpretation; the trend is eliminated after the activities are normalized to account for the fraction of CheA bound to the vesicle (Figure 2A, right). Instead, these data provide evidence for a receptor−CheW−CheA complex of increasing stability as the level of modification is increased and an activity that remains constant within the complex. Previous studies of kinase activation involving intact receptors have generally not assessed the fraction of CheA bound (*9*−*14*); in one instance where it was assessed qualitatively (*11*), the trend in complex stability as a function of covalent modification agrees with the current observations. A similar increase in stability as a function of the level of covalent modification (from EEEE to QQQQ) was also observed with soluble supramolecular signaling complexes, which were formed using Tar CF fusion proteins (and CheA and CheW) that possess an N-terminal leucine zipper dimerization motif (*36*, *48*).

CheW Dependence of Activation and Binding. The variation in the stability of the signaling complexes is also evident in the CheW dependence of CheA activity (Figure 2B) and vesicle binding (Figure 2C) for signaling complexes made

[2] The available vesicle surface area per molecule of CF was estimated to be ∼770 Å^2 using a value of 11 for the molar ratio of accessible lipid to CF and an area per molecule of 70 Å^2 for DOPC and DOGS-NTA-Ni^{2+} (*43*). The molar ratio of accessible lipid to CF was generated using the value of 60% accessibility determined by titration (see Materials and Methods) and the total lipid and protein concentrations in the sample at incubation, 280 μM DOGS-NTA-Ni^{2+}, 280 μM DOPC, and 30 μM CF. The area occupied by a close-packed CF molecule oriented end-on is estimated to be between ∼330 and ∼500 Å^2, or 2−3 times the cross-sectional area of an α-helix (∼165 Å^2, refs *44*−*46*) and is expected to result from the two α-helices in the CF coiled−coil hairpin plus unstructured polypeptide at the *c*-terminus. The area required for side-on binding is estimated to be ∼2500 Å^2 per CF molecule, in which a CF dimer occupies a rectangle defined by the approximate width (25 Å) and length (200 Å) of the dimer (*27*, *31*).

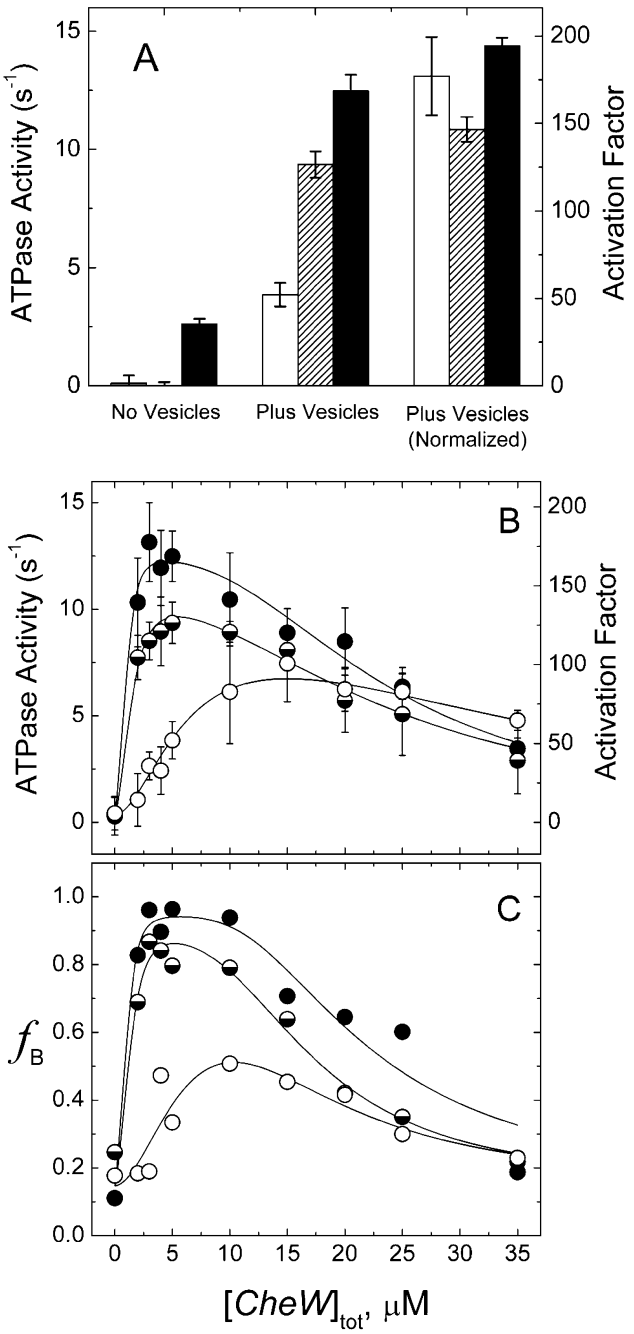

FIGURE 2: CheA activation on vesicle surfaces. (A) Left- and right-hand scales are CheA activity (s^{-1}) and the fold-increase of CheA activity in complexes relative to CheA dimers in solution, respectively. Activities (± standard error of three samples) were measured on samples (1.2 μM CheA, 5 μM CheW, and 30 μM CF) containing CF in low (EEEE), intermediate (QEQE), and high (QQQQ) modification levels (open, striped, and filled bars, respectively) in the absence of SUVs (No Vesicles, left) and with SUVs (Plus Vesicles, middle). The Plus Vesicles (Normalized) data on the right were normalized by the fraction of CheA bound to vesicles, which was determined in parallel by sedimentation. Normalized activities represent the averages of six samples (± standard error), determined at different CheW concentrations (3, 4, 5, 10, 15, and 20 μM). (B) The activity of CheA as a function of the total CheW concentration [*CheW*]$_{tot}$ and vesicle-templated CF in different modification states (EEEE, ○; QEQE, ◒; and QQQQ, ●), prepared as described in the Materials and Methods. Each point is an average of three samples (± standard deviation). (C) The fraction CheA of bound to vesicle-templated CF (f_B) as a function of [*CheW*]$_{tot}$, for CF in the three modification states (symbols as in panel B). The curves in panels B and C represent fits of the data generated as described in the text.

with CFs in the different modification states (EEEE, QEQE, and QQQQ). The rise and fall in activity and binding are consistent with the known properties of CheW, which binds both to CheA and to the receptor cytoplasmic domain (*6*, *49*). Initially, CheW facilitates an increase in the phosphotransferase and vesicle binding activities through a CF−CheW−CheA bridging interaction. Increasing the CheW concentration further leads to saturation of the binding sites on CheA and CF, and consequently, the CheA enzyme and vesicle binding activities both lessen. The relative stabilities of the CF/CheW/CheA complexes are apparent in the maximum values for activity and binding and the CheW concentrations at which these maxima occur. The CF_{QQQQ}-containing complex is judged to be most stable since it has the largest maximum values of CheA activity and binding (f_B ~0.95) at the smallest CheW concentration (<5 μM). The CF_{EEEE}-containing complex is the least stable, which is reflected in the smaller maximum values of activity and f_B (~50% of CF_{QQQQ} complexes) and the significantly larger CheW concentration at which the maximum is observed (~12 μM).

A model for complex formation, which assumes that the CheA activity is proportional to the fraction of CheA in signaling complexes bound to vesicles, f_B, captures the salient features of these data and provides preliminary estimates of the relative stability of signaling complexes as a function of covalent modification. The model is based on pairwise associations between CF (C), CheW (W), and CheA dimers (AA) according to equilibrium expressions (eqs 1−4), mass conservation relationships (eqs 5−7), and expressions for the fraction of CheA bound to vesicles (f_B, eq 8) and CheA activity (Act, eq 9). In eq 9, Act_0 and Act_{Max} are the background and maximum (100% CheA-bound) activities, respectively.

$$C + W \leftrightarrows CW \ (K_{CW}) \quad (1)$$

$$W + AA \leftrightarrows WAA \ (K_{AW}) \quad (2)$$

$$WAA + W \leftrightarrows WAAW \ (K_{AW}) \quad (3)$$

$$2C + 2W + AA \leftrightarrows CWAAWC \quad (K_{complex} = K_{CW}^2 K_{AW}^2 K_{CA}^2) \quad (4)$$

$$[C]_{tot} = [C] + [CW] + 2[CWAAWC] \quad (5)$$

$$[W]_{tot} = [W] + [AAW] + 2[WAAW] + 2[CWAAWC] \quad (6)$$

$$[AA]_{tot} = [AA] + [AAW] + [WAAW] + [CWAAWC] \quad (7)$$

$$f_B = [CWAAWC]/([AA] + [WAA] + [WAAW] + [CWAAWC]) \quad (8)$$

$$Act = Act_0 + f_B Act_{Max} \quad (9)$$

The constraints and assumptions of this model were chosen to be consistent with the experimental conditions and observations: (i) CheA was assumed to be present only as a dimer since the total CheA concentration in the samples was about 3-fold larger than the dissociation constant for

Table 1: Normalized CheA Activity and CheA and CheW Bound Fractions to Vesicles Presenting Wild-Type CFs[a]

modification level	phosphotransferase activity s^{-1} (per mol CheA bound)	fold activation[b]	f_B (CheA)	f_B (CheW)
EEEE	15.7 ± 1.6	212 ± 22	0.59 ± 0.04	0.37 ± 0.03
QEQE	10.9 ± 0.4	147 ± 5	0.83 ± 0.01	0.64 ± 0.02
QQQQ	13.2 ± 0.3	178 ± 4	0.93 ± 0.01	0.87 ± 0.01

[a] Averages and uncertainties (standard errors of the mean) were calculated from triplicate samples. Sample compositions were 30 μM CF, 560 μM total lipid (1:1 DOPC:DOGS-NTA-Ni^{2+}) in the form of SUVs, 1.2 μM CheA, and either 5 μM (CF_{QQQQ} and CF_{QEQE}) or 15 μM (CF_{EEEE}) CheW. [b] Fold activations were determined by dividing the normalized activities of CF/CheW/CheA complexes by the solution activity of 5.0 μM CheA (0.074 s^{-1}).

CheA dimerization (*39*, *40*). (ii) Direct interaction between CF and CheA was neglected in the absence of CheW since CheA exhibited small levels of binding to vesicle-templated CF in the absence of CheW (Figure 2C). (iii) The approximate proportionality between activity and f_B versus [W] data was interpreted to be consistent with a single surface-active species (CWAAWC).

The values for $[AA]_{tot}$, $[W]_{tot}$, and $[C]_{tot}$ were shared among the three sets of data (CF_{QQQQ}, CF_{QEQE}, and CF_{EEEE}) in the fits of the Act and f_B versus $[W]_{tot}$ data (Figure 2B and 2C, respectively). $[AA]_{tot}$ was fixed to the molar concentration of CheA dimer used in the experiments (0.6 μM). Act_{Max} was set to the average normalized activity (13.5 s^{-1}) observed for all three levels of modification (Figure 2A and Table 1). Act_0 was permitted to adjust in the fits, as were the individual values of the association constants. $[C]_{tot}$ was fixed to a value (10 μM) that corresponded to the CheW binding capacity of 30 μM vesicle-bound CF, which was determined in preliminary binding experiments (data not shown). A systematic analysis of the influence of $[C]_{tot}$ on the fit parameters revealed that the relative complex stabilities (e.g., $K_{complex}(QQQQ)/K_{complex}(EEEE)$) were relatively insensitive to the assigned value of $[C]_{tot}$ over a range of 10−30 μM, but the absolute values of these parameters varied.

Fits of the activity data in Figure 2B by the model and constraints described previously resulted in values for $K_{complex}$ of 1.3, 0.09, and 0.002 μM^{-4} for complexes formed with CF_{QQQQ}, CF_{QEQE}, and CF_{EEEE}, respectively, and a value for Act_0 of 0.36 ± 0.14 s^{-1}. Fits to the CheW dependence of CheA binding data (Figure 2C) generated estimates for $K_{complex}$ of 4.6, 1.0, and 0.014 μM^{-4} in CF_{QQQQ}, CF_{QEQE}, and CF_{EEEE}-containing complexes, respectively. The differences in the absolute values of $K_{complex}$ obtained from binding data, versus the estimates obtained from the activities, may illustrate in part the dependency of these parameters on the details of the model (e.g., the values chosen for $[C]_{tot}$ and Act_{Max}), which prevents useful comparisons between the absolute values of model-derived estimates for the CheA−CheW and CheW−receptor interaction constants and the measured values until the properties of vesicle-templated CFs are fully characterized. The complexity inherent in the system, including the presence of soluble and surface-bound species and possible contributions from multivalent interactions, also presents challenges for making such absolute comparisons. Nonetheless, the significant trend in $K_{complex}$, which is similar in both sets of estimates (>100-fold), reflects the change in stability of signaling complexes as a function of covalent modification. The results of a similar analysis conducted with a simpler model, in which only monovalent C−W and W−A interactions were considered to contribute to the formation of a CWA complex, also produced a significant trend (~100-fold) in the values of the constant of formation for the complex.

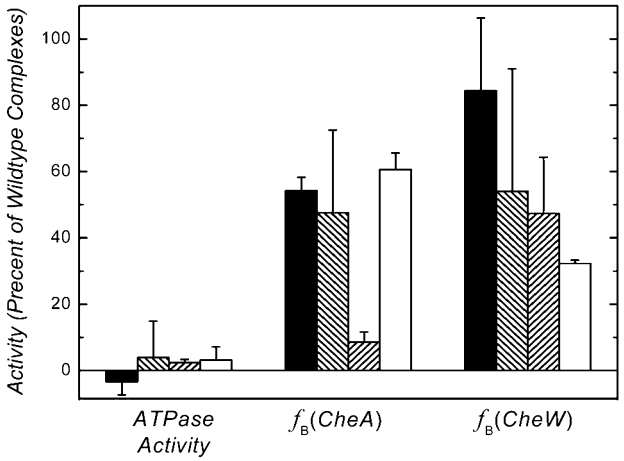

FIGURE 3: Effects of CF mutations on activity and binding. Activities and f_B are expressed as percentages relative to the complexes containing wild-type CF under the same conditions (Table 1) for the *lock-off* mutant CF:S461L (in the QEQE level of covalent modification, black bars) and the *tod* mutants CF:E383A and CF:E382P (the EEEE and QQQQ forms of CF:E383A are represented by left- and right-slanting striped bars, respectively; the QEQE form of CF:E382P is represented by open bars). Uncertainties are error-propagated values using standard errors of the mean determined on triplicate samples with the wild type and mutant complexes.

Signaling Mutations in the CF Affect CheA and CheW Binding to Various Extents. Vesicle-templated CFs are functionally similar to intact receptors in the absence of (attractant) ligand since the cytoplasmic domains activate CheA in both situations. We obtained evidence that this functional similarity is based on a common structural organization from an analysis of a limited number of *lock-off* and trimer-of-dimer (*tod*) mutations (*23*, *50*), which are located in the cytoplasmic domain at the positions shown in Figure 1. *Lock-off* mutations mimic attractant-bound ternary complexes by producing complexes that are inactive in the absence of ligand (*50*, *51*). The *lock-off* allele, a serine-461 to leucine (S461L) mutation in the intact Tar protein, is located close to the sites of methylation. The *tod* mutations, which are known to disrupt the trimer-of-dimer interaction in the homologous Tsr protein (*23*), are located near the turn in the coiled−coil hairpin. The two alleles tested correspond to the point mutations E383A and E382P in Tar. CheA and CheW binding, and also CheA activation, were measured using vesicle-templated CFs. CheA activation (Figure 3) was reduced significantly by all of these mutations, but CheA and CheW binding were retained to varying degrees, relative to wild-type CFs in the corresponding level of covalent modification (Table 1). The *lock-off* S461L CF (QEQE)

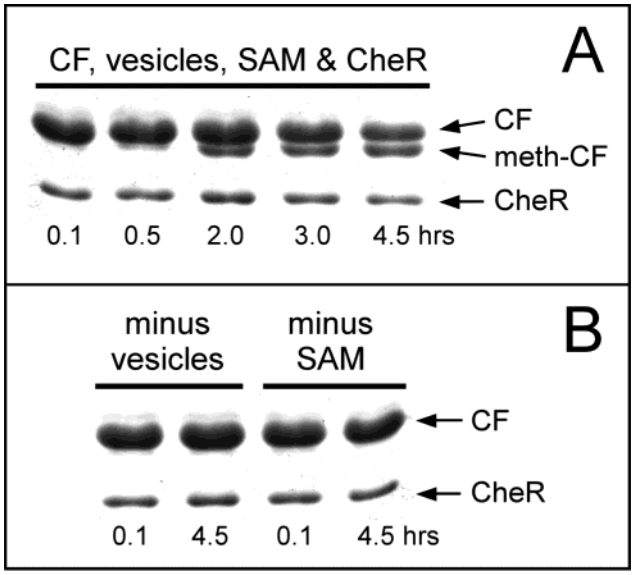

FIGURE 4: CheR-catalyzed methylation of vesicle-templated CF. (A) The change in electrophoretic mobility of methylated CF indicates the reaction progress in a sample containing CF_{EEEE}, vesicles, SAM, and CheR (~35% at 4.5 h). (B) Minus vesicle and minus SAM controls.

retained substantial binding strength overall, which is consistent with the known ability of *lock-off* mutant receptors to compete for a limited pool of CheA and CheW in mixtures with activating receptors (*51*). The lower amounts of CheA and/or CheW binding exhibited by CFs containing *tod* mutations is consistent in the disrupting effect that these types of mutations can have on the formation of receptor patches in vivo (*23*). The interference with kinase activation by the *tod* mutations is evidence that trimer-of-dimer-like interactions are also present in the vesicle-templated CFs and are necessary for CheA activation.

Surface-Assembly Enhances CF Methyl-Accepting Activity. The adaptation branch in the chemotaxis pathway involves reversible receptor methylation and demethylation, which are catalyzed by a methyltransferase and a methylesterase, respectively (*26*). Receptor methylation is a result of methyl group transfer from *s*-adenosyl-L-methionine (SAM) to specific glutamic acid residues in the cytoplasmic domain of MCPs (*52*−*54*). The process of methylation has been demonstrated to occur, at least in part, by a mechanism that involves transmethylation in which the transferase binds to the cytoplasmic domain through a tethering interaction and catalyzes methyl group transfer on a cytoplasmic domain of an adjacent receptor subunit through active site−substrate site interactions (*19*−*21*).

Surface-assembled CF can be expected to generate the close associations between cytoplasmic domains that are needed for efficient methylation via a trans mechanism. The role of surface-assembly in promoting efficient CF methylation was assessed by comparing the extent of methylation of CF on vesicle surfaces relative to CF in solution. The data in Figure 4 demonstrated that binding to the vesicle surface enhanced CF substrate activity significantly. The SDS−polyacrylamide gels in Figure 4A showed that only in the presence of vesicles, SAM, and transferase did the CF convert to a more rapidly migrating band corresponding to methylated protein. The faster migrating band was not observed in the vesicle-minus and SAM-minus controls (Figure 4B), which demonstrated that vesicle binding was required for substrate activity and that the more rapidly migrating band was not due to proteolysis of the CF, respectively. The requirement of vesicle-templating for efficient methyl group incorporation was verified by scintillation counting using tritiated SAM as the methyl group donor (data not shown).

DISCUSSION

The polyhistidine tag has found widespread use as a convenient and effective genetically encoded affinity tag for protein purification and screening applications, through the interaction of the histidine tag with metal−chelator complexes such as nickel-nitrilotriacetic acid (*55*−*57*). The histidine tag−Ni-NTA interaction has also been used in biosensor applications (*56*−*59*) and as a method for generating 2-D protein crystals when the Ni-NTA moiety is present as a headgroup in lipid monolayers (*38*, *60*−*62*). This latter use inspired us to consider it as a means to restore the functional properties of membrane-associated proteins. The results described above demonstrate the significant effect that binding receptor fragments to vesicle surfaces can have in restoring biochemical activity. Complexes of transmembrane receptors, membrane-associated adaptor proteins, and cytoplasmic enzymes are a ubiquitous feature of signaling cascades (*3*−*5*). The architecture of these complexes and their rates of assembly and disassembly are key to understanding the regulation of these biochemical processes. The vesicle-templating approach presented here should prove to be useful in such studies.

The application of this method to the bacterial chemotaxis system restores both the kinase activating and the methyl-accepting properties to the CF. On the basis of these observations, we conclude that binding to the vesicle surface promotes a lateral organization among CF subunits that resembles the organization of cytoplasmic domains in receptor-containing membranes. This conclusion is supported by the similar effects that *lock-off* and *tod* point mutations produce in templated CF and intact receptors and suggests that inter-dimer interactions (e.g., a trimer-of-dimer organization (*23*, *27*)) are critical for kinase activation. Also, the mutations appear to generate the kinase-inactive phenotype through different mechanisms, either by producing inactive complexes or by disrupting complex formation. The CF with the *lock-off* mutation retains significant CheA and CheW binding affinity while forming inactive signaling complexes; CFs with the *tod* mutations form inactive complexes at the expense of the protein−protein interaction strength to varying degrees.

The CheA activity and binding data generated with the vesicle-templated CF system demonstrate that signaling complex stability can be strongly influenced by covalent modification, and the preliminary analysis by a pairwise binding model supports this conclusion. The correlations between complex stability, CheA activation, and covalent modification in our data are consistent with previous studies of kinase activation conducted with intact receptors, which report negligible CheA activation by receptors in the lowest covalent modification level and dramatic increases as the modification is increased (*9*−*14*). These studies, which began with the ground-breaking work of Simon et al. (*9*), have been

typically conducted at relatively low concentrations of CheW (0.5−2.0 μM) and CheA (0.1−1.0 μM); concentrations that correspond to the portion of our data where the differences in CheA activity and binding between lowest and highest level of covalent modification are the greatest (Figure 2B,C; $[W]_{tot} = 2$ μM). This variation in complex stability may prove to be a significant factor in regulating kinase activity in the cell, since bacteria like *E. coli* integrate the effects of the different chemoeffector concentrations through a set of homologous receptors (*15*). CheA is the sole protein in *E. coli* through which these chemotactic responses are mediated. Therefore, regulating the extent of CheA association with (and activation by) receptors via covalent modification provides a means to weigh the response to the various chemoeffectors, which can be present simultaneously at vastly different concentrations.

ACKNOWLEDGMENT

We thank Frances Antommattei for assistance in site-directed mutagenesis of the CF, Abdalin Asinas and Tatiana Besschetnova for preparing *tod* mutants, Li Zhi for assistance with the ATPase assay, Laila Kott for purified CheW protein, and Bill Vining and Nicholas Fisher for assistance with Figure 1 artwork.

REFERENCES

1. Singer, S. J., and Nicholson, G. L. (1972) *Science 175*, 720−731.
2. Brandts, J. F., and Jacobson, B. S. (1983) *Surv. Synth. Pathol. Res. 2*, 107−114.
3. Pawson, T., and Nash, P. (2003) *Science 300*, 445−452.
4. Jordan, M. S., Singer, A. L., and Koretzky, G. A. (2003) *Nat. Immmunol. 4*, 110−116.
5. Sheng, M., and Sala, C. (2001) *Annu. Rev. Neurosci. 24*, 1−29.
6. Gegner, J. A., Graham, D. R., Roth, A. F., and Dahlquist, F. W. (1992) *Cell 70*, 975−982.
7. Schuster, S. C., Swanson, R. V., Alex, L. A., Bourret, R. B., and Simon, M. I. (1993) *Nature 365*, 343−347.
8. Borkovich, K. A., Kaplan, N., Hess, J. F., and Simon, M. I. (1989) *Proc. Natl. Acad. Sci. U.S.A. 86*, 1208−1212.
9. Borkovich, K. A., Alex, L. A., and Simon, M. I. (1992) *Proc. Natl. Acad. Sci. U.S.A. 89*, 6756−6760.
10. Barnakov, A. N., Barnakova, L. A., and Hazelbauer, G. L. (1998) *J. Bacteriol. 180*, 6713−6718.
11. Li, G., and Weis, R. M. (2000) *Cell 100*, 357−365.
12. Bornhorst, J. A., and Falke, J. J. (2000) *Biochemistry 39*, 9486−9493.
13. Levit, M. N., and Stock, J. B. (2002) *J. Biol. Chem. 277*, 36760−36765.
14. Bornhorst, J. A., and Falke, J. J. (2003) *J. Mol. Biol. 326*, 1597−1614.
15. Adler, J. (1975) *Annu. Rev. Biochem. 44*, 341−356.
16. Maddock, J. R., and Shapiro, L. (1993) *Science 259*, 1717−1723.
17. Sourjik, V., and Berg, H. C. (2000) *Mol. Microbiol. 37*, 740−751.
18. Cantwell, B. J., Draheim, R. R., Weart, R. B., Nguyen, C., Stewart, R. C., and Manson, M. D. (2003) *J. Bacteriol. 185*, 2354−2361.
19. Wu, J., Li, J., Li, G., Long, D. G., and Weis, R. M. (1996) *Biochemistry 35*, 4984−4993.
20. Li, J., Li, G., and Weis, R. M. (1997) *Biochemistry 36*, 11851−11857.
21. Le Moual, H., Quang, T., and Koshland, D. E., Jr. (1997) *Biochemistry 36*, 13441−13448.
22. Gestwicki, J. E., and Kiessling, L. L. (2002) *Nature 415*, 81−84.
23. Ames, P., Studdert, C. A., Reiser, R. H., and Parkinson, J. S. (2002) *Proc. Natl. Acad. Sci. U.S.A. 99*, 7060−7065.
24. Le Moual, H., and Koshland, D. E., Jr. (1996) *J. Mol. Biol. 261*, 568−585.
25. Zhulin, I. B. (2001) *Adv. Microbiol. Physiol. 45*, 157−198.
26. Springer, M. S., Goy, M. F., and Adler, J. (1979) *Nature 280*, 279−284.
27. Kim, K. K., Yokota, H., and Kim, S.-H. (1999) *Nature 400*, 787−792.
28. Milburn, M. V., Privé, G. G., Milligan, D. L., Scott, W. G., Yeh, J., Jancarik, J., Koshland, D. E., Jr., and Kim, S.-H. (1991) *Science 254*, 1342−1347.
29. Yeh, J. I., Biemann, H. P., Privé, G. G., Pandit, J., Koshland, D. E., Jr., and Kim, S.-H. (1996) *J. Mol. Biol. 262*, 186−201.
30. Falke, J. J., Bass, R. B., Butler, S. L., Chervitz, S. A., and Danielson, M. A. (1997) *Annu. Rev. Cell Dev. Biol. 13*, 457−512.
31. Weis, R. M., Hirai, T., Chalah, A., Kessel, M., Peters, P. J., and Subramaniam, S. (2003) *J. Bacteriol. 185*, 3636−3643.
32. Ninfa, E. G., Stock, A., Mowbray, S., and Stock, J. (1991) *J. Biol. Chem. 266*, 9764−9770.
33. Bogonez, E., and Koshland, D. E., Jr. (1985) *Proc. Natl. Acad. Sci. U.S.A. 82*, 4891−4895.
34. Ames, P., and Parkinson, J. S. (1994) *J. Bacteriol. 176*, 6340−6348.
35. Cochran, A. G., and Kim, P. S. (1996) *Science 271*, 1113−1116.
36. Liu, Y., Levit, M., Lurz, R., Surette, M. G., and Stock, J. B. (1997) *EMBO J. 16*, 7231−7240.
37. Francis, N. R., Levit, M. N., Shaikh, T. R., Melanson, L. A., Stock, J. B., and DeRosier, D. J. (2002) *J. Biol. Chem. 277*, 36755−36759.
38. Schmitt, L., Dietrich, L., and Tampé, R. J. (1994) *J. Am. Chem. Soc. 166*, 8485−8491.
39. Kott, L., Braswell, E. M., Shrout, A. L., and Weis, R. M. (2003) *Biochim. Biophys. Acta*, in press.
40. Surette, M. G., Levit, M., Liu, Y., Lukat, G., Ninfa, E. G., Ninfa, A., and Stock, J. B. (1996) *J. Biol. Chem. 271*, 939−945.
41. Norby, J. G. (1988) *Methods Enzymol. 156*, 116−119.
42. Press, W. H., Flannery, B. P., Teukolsky, S. A., and Vetterling, W. T. (1986) *Numerical Recipes. The Art of Scientific Computing*, pp 523−528, Cambridge University Press, Cambridge.
43. Nagle, J. F., and Tristram-Nagle, S. (2000) *Biochim. Biophys. Acta 1469*, 159−195.
44. Luecke, H., Schobert, B., Richter, H. T., Cartailler, J. P., and Lanyi, J. K. (1999) *J. Mol. Biol. 291*, 899−911.
45. Ren, G., Reddy, V. S., Cheng, A., Melnyk, P., and Mitra, A. K. (2001) *Proc. Natl. Acad. Sci. U.S.A. 98*, 1398−1403.
46. Heymann, J. A. W., Sarker, R., Hirai, T., Shi, D., Milne, J. L. S., Maloney, P. C., and Subramaniam, S. (2000) *EMBO J. 20*, 4408−4413.
47. Dunten, P., and Koshland, D. E., Jr. (1991) *J. Biol. Chem. 266*, 1491−1496.
48. Levit, M. N., Liu, Y., and Stock, J. B. (1999) *Biochemistry 38*, 6651−6658.
49. Boukhvalova, M. S., Dahlquist, F. W., and Stewart, R. C. (2002) *J. Biol. Chem. 277*, 22251−22259.
50. Mutoh, N., Oosawa, K., and Simon, M. I. (1986) *J. Bacteriol. 167*, 992−998.
51. Borkovich, K. A., and Simon, M. I. (1990) *Cell 63*, 1339−1348.
52. Kehry, M. R., and Dahlquist, F. W. (1982) *J. Biol. Chem. 257*, 378−386.
53. Terwilliger, T. C., and Koshland, D. E., Jr. (1984) *J. Biol. Chem. 259*, 7719−7725.
54. Kehry, M. R., Engstrom, P., Dahlquist, F. W., and Hazelbauer, G. L. (1983) *J. Biol. Chem. 258*, 5050−5055.
55. Crowe, J., Dobeli, H., Gentz, R., Hochuli, E., Stuber, D., and Henco, K. (1994) *Methods Mol. Biol. 31*, 371−387.
56. Jones, C., Patel, A., Griffin, S., Martin, J., Young, P., O'Donnell, K., Silverman, C., Porter, T., and Chaiken, I. (1995) *J. Chromatogr., A 707*, 3−22.
57. Terpe, K. (2003) *Appl. Microbiol. Biotechnol. 60*, 523−533.
58. Nieba, L., Nieba-Axmann, S. E., Persson, A., Hamalainen, M., Edebratt, F., Hansson, A., Lidholm, J., Magnusson, K., Karlsson, A. F., and Pluckthun, A. (1997) *Anal. Biochem. 252*, 217−228.
59. Gershon, P. D., and Khilko, S. (1995) *J. Immunol. Methods 183*, 65−76.
60. Frey, W., Schief, W. R., Jr., Pack, D. W., Chen, C. T., Chilkoti, A., Stayton, P., Vogel, V., and Arnold, F. H. (1996) *Proc. Natl. Acad. Sci. U.S.A. 93*, 4937−4941.
61. Celia, H., Wilson-Kubalek, E., Milligan, R. A., and Teyton, L. (1999) *Proc. Natl. Acad. Sci. U.S.A. 96*, 5634−5639.
62. Thess, A., Hutschenreiter, S., Hofmann, M., Tampé, R., Baumeister, W., and Guckenberger, R. (2002) *J. Biol. Chem. 277*, 36321−36328.

BI0352769